

Pentavalent vanadium ion addition to Ni–Zn ferrites

Part 2 *Electrical conductivity*

RAM NARAYAN, R. B. TRIPATHI, B. K. DAS, G. C. JAIN

Division of Materials, National Physical Laboratory, New Delhi 110 012, India

The d.c. and a.c. electrical conductivities of iron-excess and iron-deficient compositions of Ni–Zn ferrites, with varying V_2O_5 content sintered at different temperatures (1200 to 1300°C) for 2 h in air, has been studied. The electrical conductivity increased with a 0.2 mol % addition of V_2O_5 . The minimum d.c. and a.c. electrical conductivities were found at a V_2O_5 content of 0.4 mol % followed by a small increase for still higher concentrations of V_2O_5 (≥ 0.6 to 1.0 mol %). The minima at 0.4 mol % were unaffected by the sintering temperature in both the iron-excess and iron-deficient cases. The activation energies for a.c. conduction at 1 MHz were always less than the corresponding values for d.c. conduction. The results obtained can be explained in terms of solubility of V_2O_5 , which creates ferrous ions and localizes Fe^{2+} ions by forming triplets in the ferrite matrix.

1. Introduction

Because of low electrical conductivity, ferrites have an advantage over other magnetic materials, particularly at higher frequencies. The pioneering work of Verway and De Boer [1] showed that electrical conduction in ferrites can be explained by the charge exchange between the multiple valence ions of the same atom, present at equivalent lattice sites. Electrical conduction in Fe_3O_4 has been explained on the basis of the hopping polaron model [2]. Electrical conductivity has been significantly influenced by additives. Influence of tetravalent ions, Sn^{4+} and Ti^{4+} , in Mn–Zn ferrites [3–5] and bivalent ions, Mn^{2+} and Co^{2+} , in Ni–Zn ferrites [6] has been much discussed. The work reported in this paper aims at understanding the role of high valence ions (V^{5+}) in controlling the magnetic loss factor via modification of electrical conductivity. The data obtained on the temperature variation of V_2O_5 -doped and V_2O_5 -undoped Ni–Zn ferrites has been presented. Preliminary work on this subject has been published elsewhere [7].

2. Experimental procedures

Sets of iron-excess and iron-deficient Ni–Zn

ferrites were prepared by the method described in Part 1 of this paper [8]. For the characterization of samples, techniques of X-ray diffraction (XRD), optical metallography and electron probe microanalysis (EPMA) were used.

Indium–mercury amalgam was rubbed on both sides of each tablet to give a uniform coating of the amalgam required for ohmic contact. The d.c. bulk resistivity was measured at an applied field of one $mV\text{cm}^{-1}$ by the two-probe contact method using a d.c. microvoltmeter and picoammeter. The four-probe method was also used to measure the d.c. resistivity, but there were no differences in results between this method and the two-probe method if indium–mercury amalgam was used as the contact material. The temperature variation (25 to 100°C) of conductivity was measured by heating the sample in a small oven and keeping it at a stable temperature for about 2 h to avoid any temperature gradient inside the sample. The a.c. conductivity at 1 MHz was measured by an impedance bridge (Siemen's R 2077) using the two-probe method.

3. Results

The X-ray Debye–Scherrer powder pattern of the

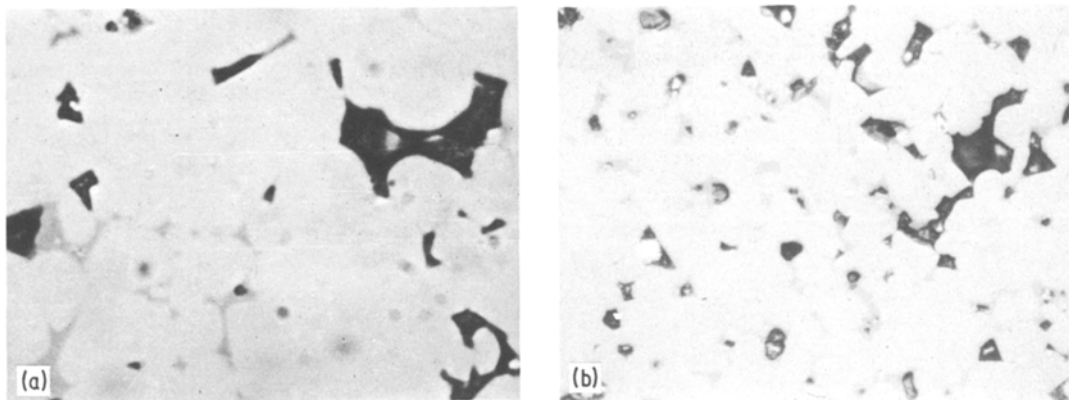


Figure 1 Microstructure of polished surface of (a) iron-deficient (b) iron-excess compositions, containing 1 mol% V_2O_5 , sintered at 1200°C for 2 h in air. Magnification $\times 702$.

samples showed that a single phase was present in all the samples studied. The lattice parameter was also found to be unaffected by the addition of V_2O_5 [8]. Figs. 1a and b show photographs of a well polished surface of iron-excess and iron-deficient Ni–Zn ferrites, respectively, containing 1 mol% V_2O_5 . A distinct grey coloured second phase could be seen at the grain boundaries and at the points where three or more grains meet. However, this phase could not be detected by XRD measurements. The grey coloured second

phase seen in the optical photomicrograph of polished surface was analysed by EPMA. Fig. 2 shows the result of X-ray microanalysis (area scan) for vanadium of an iron-excess (IE) composition containing 1 mol% V_2O_5 . It is clearly indicated by this figure that a vanadium-rich second phase was present along the grain boundaries in this sample. Such a second phase was also present in the iron-deficient (ID) composition samples.

The d.c. conductivity of IE and ID compositions, sintered at different temperatures (1200 to 1300°C) for 2 h in air, has been plotted as a function of V_2O_5 concentration in Figs. 3a and b. For both IE and ID compositions the electrical conductivity increased for a V_2O_5 content of 0.2 mol%. At higher V_2O_5 content (0.4 mol%) it decreased sharply to a very low value followed by a small increase for still higher concentrations of V_2O_5 (0.6 to 1.0 mol%). Figs. 4a and b depict variations in a.c. conductivities with V_2O_5 content for IE and ID compositions sintered at different temperatures (1200 to 1300°C). The activation energies of conduction obtained from $\log(\sigma T)$ against $1/T$ plots for these samples have been listed in Table I. For both the IE and ID compositions the activation energy was found to be a maximum for samples containing 0.4 mol% V_2O_5 . For all samples the activation energies of conduction at 1 MHz were less than the corresponding values for d.c. conduction. Fig. 5 shows the variation of electrical conductivity and dielectric constant of 1.0 mol% of V_2O_5 with frequency. Dispersion was observed well below 1 MHz. The conductivity of the materials remained more or less constant after 1 MHz as did the dielectric constant.

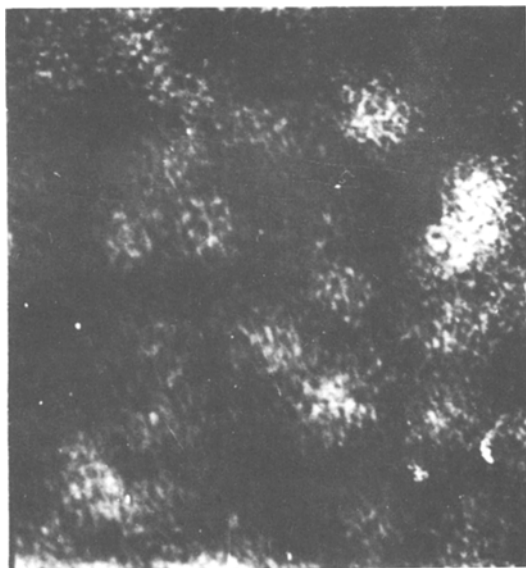


Figure 2 Characteristic X-ray image from XMP analysis of an iron-excess ferrite containing 1 mol% of V_2O_5 , sintered at 1200°C for 2 h in air showing concentration of vanadium at grain boundaries.

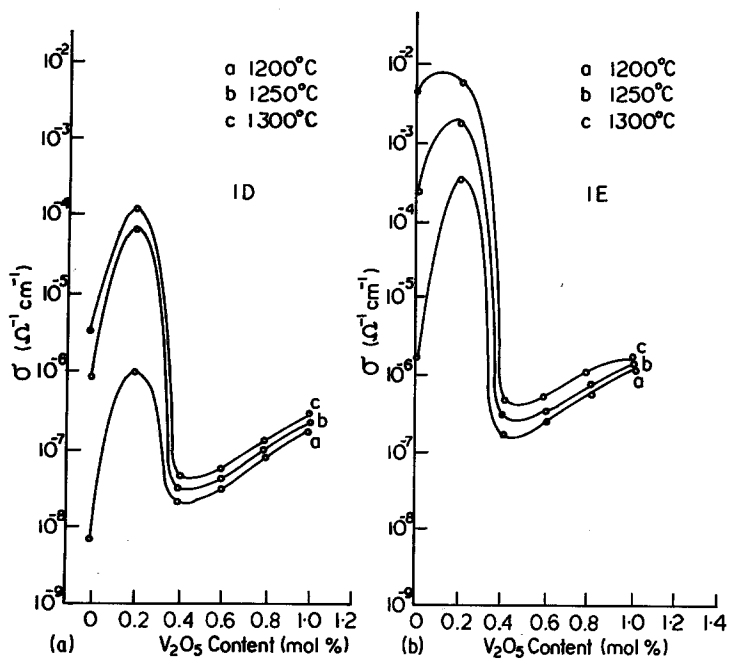


Figure 3 The d.c. conductivity plotted against V_2O_5 content for (a) iron-deficient and (b) iron-excess compositions sintered at various temperatures for 2 h in air.

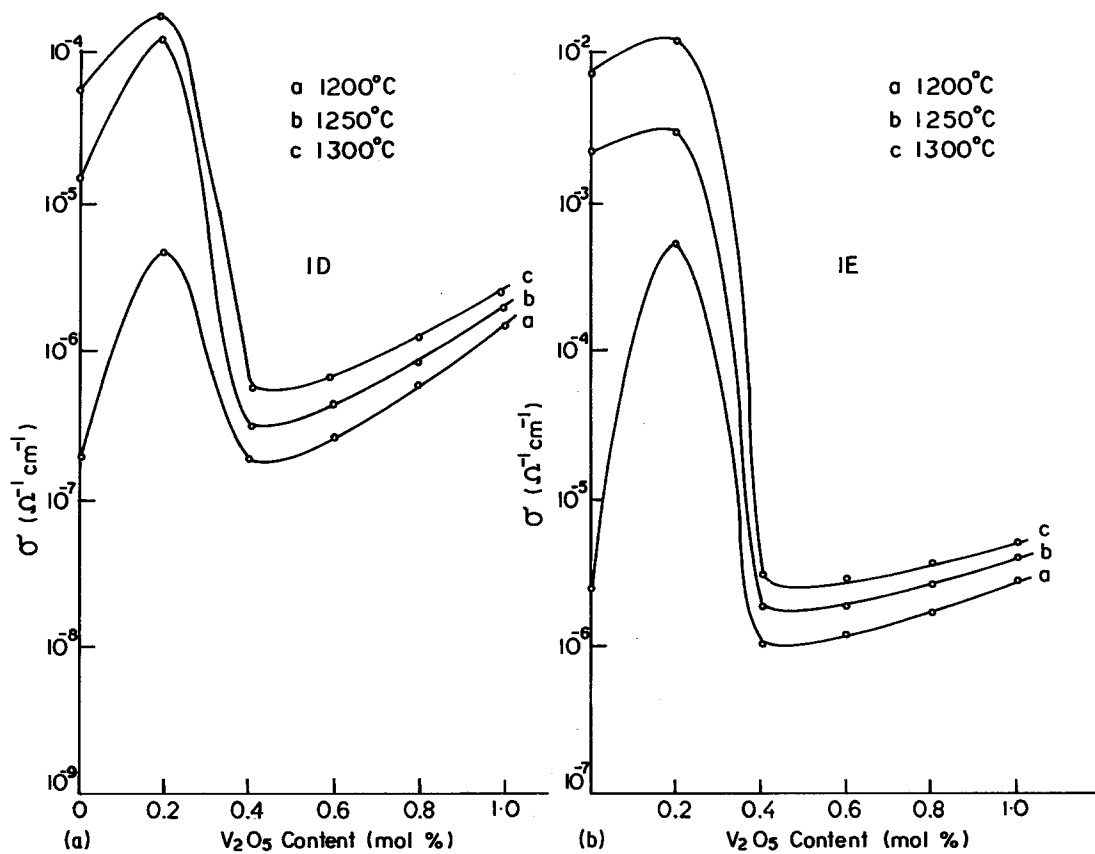


Figure 4 The a.c. conductivity at 1 MHz plotted against V_2O_5 content for (a) iron-deficient and (b) iron-excess compositions sintered at various temperatures for 2 h in air.

TABLE I Activation energy of d.c. and high-frequency (1 MHz) electrical conduction of iron-deficient and iron-excess Ni–Zn ferrites for various V₂O₅ contents (sintering temperature is 1250° C)

V ₂ O ₅ content (mol %)	Activation energy of conduction (eV)			
	Iron-deficient		Iron-excess	
	d.c.	1 MHz	d.c.	1 MHz
0.0	0.28 ± 0.02	0.21 ± 0.02	0.25 ± 0.02	0.18 ± 0.02
0.2	0.27 ± 0.02	0.19 ± 0.02	0.26 ± 0.02	0.20 ± 0.02
0.4	0.39 ± 0.02	0.27 ± 0.02	0.36 ± 0.02	0.27 ± 0.02
1.0	0.40 ± 0.02	0.27 ± 0.02	0.35 ± 0.02	0.27 ± 0.02

4. Discussion

The data obtained in the present studies for variation of conductivity (σ) with temperature (T) fits well in the equation

$$\sigma(T) = C/T \exp(-E/kT) \quad (1)$$

where k is the Boltzmann constant. The present findings also reveal that for the same V₂O₅ content the iron-excess ferrites have smaller activation energies of conduction than the iron-deficient ones. It has been found experimentally that the said ferrites' compositions exhibit n-type electrical conductivity, and that therefore the electrical conduction is due to electron hopping between Fe²⁺ and Fe³⁺ ions. In iron-excess ferrites, the carrier concentration (Fe²⁺ ions) is more compared to that in iron-deficient ferrites. Thus the activation energy for electrical conduction decreases with the increase in carrier concentration. It has been found by Koops [10] as well as by the authors (see Fig. 5) that dispersion in Ni–Zn ferrites occurs below 1 MHz. Therefore, the resistivity at 1 MHz can be considered as high-frequency resistivity, which is equal to the grain resistivity. The main contribution to the d.c. resistivity comes from the grain boundary resistivity [10]. The grain boundaries contain less Fe²⁺ ions than the interior of the grains due to the preferential oxidation of grain boundaries during cooling, and hence have fewer carriers than the grain interior. This leads to a higher activation energy for d.c. conduction compared to that for a.c. conduction.

It is found that the electrical conductivity increases with a small addition (0.2 mol%) of V₂O₅. It has also been found that V₂O₅ is partially soluble in Ni–Zn ferrites [9]. The dissolution of V₂O₅ into the spinel lattice leads to the creation of divalent iron and cation vacancies.

The increase in conductivity with the addition of 0.2 mol% V₂O₅ and the disaccommodation data

of V₂O₅-doped Ni–Zn ferrites [11] leads to the conclusion that with the addition of V₂O₅ up to the solubility limit, the Fe²⁺ ion concentration increases. However, the oxidation–reduction equilibrium for iron requires that in the absence of any other charge an increase in cation vacancy accompanies an increase in the (Fe²⁺)/(Fe³⁺) ratio. Johnson *et al.* [12] also reached a similar conclusion by estimating quantitatively the vacancy and Fe²⁺ ion concentration with increasing amounts of Ti⁴⁺ ions in the single phase Mn–Zn ferrites. Thus, as discussed earlier, for every addition of a V⁵⁺ ion 7/3 Fe³⁺ ions are reduced to 7/3 Fe²⁺ ions. It can also be hypothesized that V⁵⁺ ions localize Fe²⁺ ions forming V⁵⁺ < $\begin{smallmatrix} \text{Fe}^{2+} \\ \text{Fe}^{2+} \end{smallmatrix}$ triplets analogous to Ti⁴⁺–Fe²⁺ pairs in the case of titanium-substituted Mn–Zn ferrites. Thus 3 V⁵⁺ ions produce 7 Fe²⁺ ions and localize six of them forming three triplets and hence depriving them from taking part in conduction. Therefore, for each incorporation of 3 V⁵⁺ ions into the lattice one extra Fe²⁺ ion will be available for conduction. This leads to an increase in the grain conductivity and hence the bulk conductivity of the ferrite, as observed in the present studies with the addition of 0.2 mol% V₂O₅. Moreover, the grain size, the density and the microstructure also influence the bulk conductivity of the material. Incorporation of V⁵⁺ ions into the lattice brings about changes in the system and the corresponding effects on conductivity are as listed below.

1. It increases the Fe²⁺ ion concentration which in turn increases the conductivity.

2. It changes the grain size, density and microstructure as can be seen from Part 1 of this paper [8].

(a) An increase in the grain size will increase the bulk conductivity.

(b) An increase in the density will increase the bulk conductivity by suppressing preferential oxidation of the grain boundaries. Presence of the

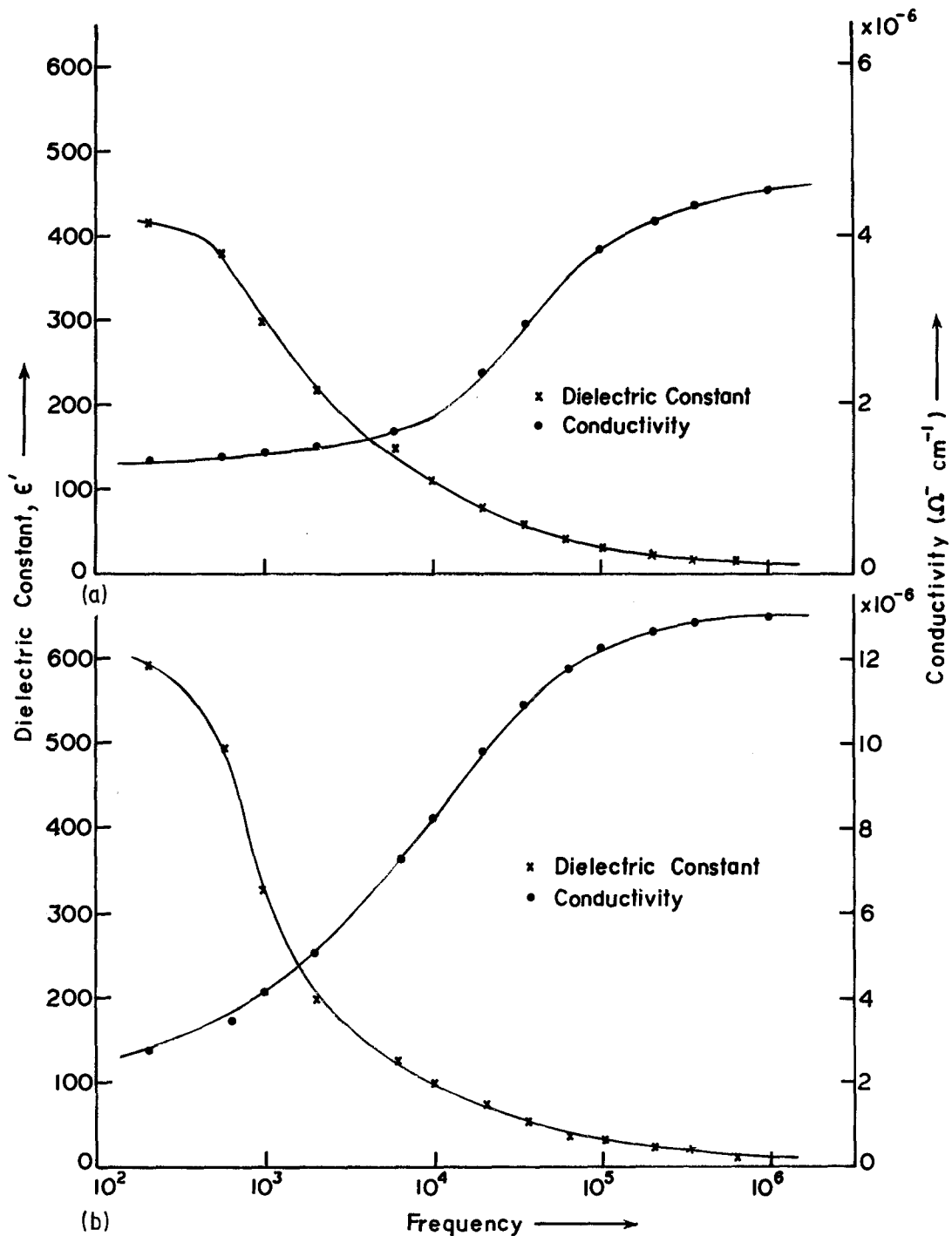


Figure 5 Dielectric constant and electrical conductivity plotted against frequency for (a) iron-deficient and (b) iron-excess compositions containing 1 mol % V_2O_5 sintered at 1250°C for 2 h in air.

closed or open pores at grain boundaries facilitates oxidation of the grain boundaries during cooling after sintering. The changes in density of Ni-Zn doped with V_2O_5 has been explained.

(c) The intergranular porosity will decrease

the conductivity by oxidizing locally the regions around pores, thereby effectively increasing the grain resistivity. The intergranular porosity has been discussed in Part 1 of this paper [8].

3. V^{5+} ions entering into the lattice may segregate

gate near the grain boundaries thereby increasing its effective thickness and so decreasing the bulk conductivity. Segregation of titanium at the grain boundaries in the Mn–Zn ferrite has been detected by Auger spectroscopy [13].

In the case of the iron-deficient composition the increase in the conductivity with addition of 0.2 mol% V_2O_5 is of a few orders of magnitude, whereas in the case of the iron-excess composition the increment is only of a factor of 1 to 5 (for a sintering temperature of 1250° C). This is because in the basic iron-deficient composition the Fe^{2+} ion concentration is negligibly small. Therefore, a small increase in Fe^{2+} ions concentration in the lattice brings about a large change in the Fe^{2+}/Fe^{3+} ratio, thereby changing the conductivity by several orders of magnitude. In the case of iron-excess composition, the Fe^{2+} ions concentration is quite large, so a small increase in Fe^{2+} ion concentration due to addition of 0.2 mol% V_2O_5 results in a small relative change in the Fe^{2+}/Fe^{3+} ratio, leading to a small relative increase in the conductivity. At the lower sintering temperature of 1200° C, the Fe^{2+} ion content is much less even in the basic iron-excess ferrite and therefore, the increase in Fe^{2+} ion concentration due to addition of 0.2 mol% V_2O_5 brings about a large relative increase in the Fe^{2+}/Fe^{3+} ratio and hence in the conductivity, as observed in the present studies. A sharp increase in the electron conductivity was also observed by Sokalov and Fedorova [14] in the case of an iron-excess Ni–Zn–Co ferrite when the sintering temperature was increased beyond 1200° C.

With an increase in V_2O_5 addition to 0.4 mol %, a sharp decrease in conductivity is observed in both the iron-excess and iron-deficient ferrites. The increase in the Fe^{2+} ion concentration due to additional V^{5+} ions will not change the Fe^{2+}/Fe^{3+} ratio much due to the reasons discussed earlier. The high-frequency data (see Figs. 4a to b) reveal a sharp decrease in grain conductivity in these specimens. This is because in these samples the V^{5+} ions occupy octahedral sites and hence V^{5+} ions apart from localizing Fe^{2+} ions, behave as scattering centres for hopping electrons, consequently decreasing their mobility and therefore the grain conductivity. The increase in activation energy of d.c. and high-frequency electrical conductivity (see Table I) in these samples can also be attributed to scattering effects. Brabers [15] has reported that in the case of manganese ferrous

ferrites, the electrical conductivity decreases if there is an increase in the degree of inversion, i.e. an increase in Mn^{2+} ions at octahedral sites. According to him Mn^{2+} ions at octahedral sites behave as scattering centres for hopping electrons, thereby decreasing the conductivity. The increased activation energy of electrical conduction in the case of the heavily titanium-substituted Mn–Zn ferrites and the increase in the activation energy of conduction in $Fe_{3-x}Ti_xO_4$ [16] with increasing x has also been attributed to scattering effects due to the created octahedral Ti^{4+} ions. Moreover, V^{5+} ions segregate towards grain boundaries. The oxidized grain boundary would not contain more scattering centres and hence the electrical conductivity of the grain boundary layer would decrease on addition of V^{5+} ions thereby decreasing the d.c. conductivity.

With a further increase in V_2O_5 concentration to 1 mol % an increase in the conductivity is observed in both the ferrite compositions. This can be attributed to the increased grain size, as was observed in Part 1 of this paper [8]. Moreover, in these samples a second phase rich in vanadium precipitates at grain boundaries (see Figs. 1 and 2) and this probably increases the grain boundary conductivity and hence the bulk conductivity, as observed in these composition.

5. Conclusions

The following conclusions may be drawn from the present studies.

1. Conduction in ferrites is due to charge transport by hopping electrons.
2. Within solubility limits an increase in the amount of V_2O_5 leads to an increase in the Fe^{2+} ion content and cation vacancies.
3. The presence of V^{5+} ions in the ferrite matrix results in the formation of $V^{5+} < \begin{smallmatrix} Fe^{2+} \\ Fe^{2+} \end{smallmatrix}$ triplets and increased scattering of electrons at higher vanadium concentrations.

Acknowledgements

The authors wish to express their appreciation to Dr A. R. Verma, Director, National Physical Laboratory, for granting permission to publish this work.

References

1. E. J. W. VERWAY and J. H. DE BOER, *Rec. Trav. Chim. Pays Bas* 55 (1936) 531.
2. W. HAUBENREISSER, *Phys. Status Solidi* 1 (1961) 619.

3. D. S. TANNHAUSER, *Phys. Kondensierten Mater.* **3** (1964) 146.
4. I. HANKE and M. ZENGER, *J. Magn. Magn. Mater.* **4** (1977) 120.
5. V. A. M. BRABERS, *Appl. Phys.* **9** (1976) 347.
6. Y. KAWAI, M. TANOBE and T. OGAWA, *Phys. Status Solidi (a)* **55** (1979) K55.
7. G. C. JAIN, B. K. DAS, R. B. TRIPATHI and RAM NARAYAN, *IEEE Mag.* **18** (1982) 776.
8. RAM NARAYAN, R. B. TRIPATHI and B. K. DAS, *J. Mater. Sci.* **18** (1983) 1267.
9. *Idem*, *J. Magn. Magn. Mater.* **14** (1979) 80.
10. G. G. KOOPS, *Phys. Rev.* **83** (1951) 121.
11. G. C. JAIN, B. K. DAS, R. B. TRIPATHI and RAM NARAYAN, *Phys. Status Solidi (a)* **57** (1980) K105.
12. D. W. JOHNSON Jr, P. K. GALLAGHER, M. F. YON and H. SCHRIEBER, *J. Solid State Chem.* **30** (1979) 229.
13. P. E. C. FRANKEN, H. VAN DOVEREN and J. A. T. VERHOEVEN, *Cermergia Inst.* **3** (3) (1967) 122.
14. A. D. SOKALOV and M. N. FEDOROVA, *Phys. Met. Metall.* **22** (1966) 169.
15. V. A. M. BRABERS, *Appl. Phys.* **9** (1976) 347.
16. S. K. BANERJEE, W. O. REILLY, T. C. GIBB and N. N. GREENWOOD, *J. Phys. Chem. Solids* **28** (1967) 1323.

Received 23 April

and accepted 23 September 1982